ANNALS OF ANATOMY

# Quantitative investigations into the histostructural nature of the human putamen

## II. The differentiated topological distribution of certain neuron type arrangements

**O. Schmitt*, R. Eggers and H. Haug**

Institute of Anatomy, Medical University of Lübeck, Ratzeburger Allee 160, D-23538 Lübeck, Germany

**Summary.** Several mathematical procedures have been worked out for describing quantitave arrangements of neurons, and especially subpopulations of neurons, in the human putamen. Visual point field analysis is a newly developed method for the qualitative recognition of the fuzzy clustering of types of neurons. Nearest neighbourhood analysis is an established procedure in stochastic geometry and image analysis. These cluster-analytical methods make possible the determination of local neuron topology. They represent an extension and application of the point pattern analysis (Diggle 1983), and are used here to calculate the statistical significance of certain arrangements of cells.

The application of all these methods together revealed an interesting neuronal arrangement: type 1 neurons tend to remain at a certain distance from other type 1 neurons, whereas type 6 neurons lie close together.

**Key words:** Putaman – Human – Topology – Morphometry – Point pattern analysis – Neuron arrangements – Cytoarchitectonic – Structural evaluation – Cluster analysis – Stochastic geometry – Spatial distribution

## Introduction

So far only a few studies have been reported in which structural parameters *between* cells have been systematically determined (Mariani et al. 1984; Braendgaard and Gundersen 1986; Benes et al. 1987; Rother et al. 1987; Ranke et al. 1989). These structural parameters are essential for the characterization of assemblies of cells.

The quantitative investigation of spatially distributed objects, e.g. neurons, is generally called stochastic geometry (Rogers 1974; Harding and Kendall 1974; Davis and McCullagh 1975; Getis and Boots 1978; Tautu 1984; Upton and Fingleton 1985; Stoyan et al. 1987; Böker 1987; Mecke et al. 1990; Karr 1991; König and Schmidt 1992; Stoyan 1993; Ambartzumjan et al. 1993). We used certain well known applications of the stochastic geometry which were developed by Diggle (1983), and also describe here other methods of quantifying spatially distributed objects.

We have called this analytical approach *structure analysis* (SCA) because we used it to investigate the spatial distribution of structural elements. In this case the neurons or other cells are the elements, and their distribution in the tissue is the structure.

Generally we used only a few procedures of the stochastic geometry. For the sake of completion, we include further techniques which are usefull for investigating biological material. The data may consist of morphometric variates or be obtained from video images.

1. Texture analysis is used to describe the periodicity of structures on the surface, or in sections of biological specimens.
2. Point pattern analysis, a subdivision of stochastic geometry, can be used to characterize the statistically fuzzy distribution of various types of cells.
3. Tesselation methods (Voronoi, Delauny) are also used in stochastic geometry for modelling and for quantitative characterization of static and dynamic intercellular regions.
4. Multivariate statistics, including in particular the different models of cluster analysis, is available for deter-

* This paper represents a portion of a thesis in fullfilment for the degree of Dr. med. presented by Oliver Schmitt to the Medical Faculty, Medical University of Lübeck.

Correspondence to: O. Schmitt

ming discretely distributed entities within histological specimens.

5. The techniques of fuzzy logic pattern recognition make it possible to detect specified point arrangements or cell distributions.
6. Artificial neural networks can be constructed for the recognition of typical features within point patterns.

We have found these methods of great importance for anatomical research and, in particular, for quantitative cytoarchitectonics of nervous tissue. By means of SCA we have been able to find parameters for the quantitative description of complex structures such as cellular arrangements, and to compare normal, with pathological and developing tissues.

In addition we discovered neuron compositions which provide an insight into the possible functional interrelationships of certain arrangements of cells.

## Material and methods

In a previously published section of this article (Schmitt et al. 1995), we described the specimens, staining methods and morphometric technique employed for investigating 27 human putamina. In 14 of these the investigation involved 7 entirely different types of neuron.

The basic stereologic parameters having been calculated by a modular developed Pascal program (MORPHON) on ×86 PC's equipped with MS-DOS®. These were used for the quantitative evaluations about to be described.

The terms 'points' and 'events' used here refer to 'cell' or 'neuron'.

Weighted coordinates of the different types of neuron (**o**riginal **d**ata = **o**bserved **d**ata: OD) were plotted before using SCA, in order to get a visual impression of the distribution of the types of neuron (Haug 1979). Examples of these are shown in Fig. 2, and will be described later (see "Results").

These plotts were then used to identify the local distribution of certain types of neuron. This technique is known as *visual point field analysis* (VPA). The results of such analysis are shown in Fig. 2 and will be described later. The second stage of the SCA methods is known as *nearest neighbourhood analysis* (NNA). The cell gravity centers of the neuron types are again used, but in a completely different manner from that of VPA. Each neuron is iteratively combined with every type of cell separately. Such a combination of two objects (in this case two neurons) is described in mathematical terms as 'n-tuple' (n = 2 if only two neurons are combined). Here the term refers to the relationship of one type of neuron (x) to another type (y). This also includes a tuple of identical types: e. g. tuple 11 is a combination of a type 1 with another type 1 neuron of the same type.

Only the least distance between two neurons is stored. With these values we examined statistically the frequency of cell types in every nearest neighbourhood, including the tuple within the same population. We also determined the neurons within the tuple were lying significantly closer together than to those of any other tuple. For example, are the type 6 neurons lying closer to each other than to type 1 neurons?

Equation (1) was used to estimate the distance to the nearest gravity center. In order to examine the kind of cell distribution, the OD were compared with pseudorandomized cell populations of equal size (RDC: randomized data of cell gravity center). The differences between OD and RDC were compared by the Dixon-Mood-test (DMT), the Kolmogoroff-Smirnoff-test (KST) and the U-test, with NULL-hypothesis of a randomized neuron distribution.

We also examined the vicinity between the gravity coordinates of different tuple by *neighbourhood cluster analysis* (NCA) and *contact cluster analysis* (CCA) (Fig. 1), using a different method of combination (Schmitt 1991). We introduced the symbol V to represent a feature vector of the measurement for every single neuron. This includes the gravity center, maximal diameter, projection area and spherical index. The latter provides a parameter for deviation of the real shape from an ideal circle. It is a product of the planimetric area and the cell diameter.

The feature vector V: $(x_i,y_i)$ is combined with every other cell feature vector. We systematically selected neuron types which we did not exspect to be randomly distributed.

The basic distance $B_I$ (or in vector form: $d(V_i; V_j)$) is calculated by using formula (1) and represents Euclidean distance. These values of the OD were compared with three artificially generated cell distributions. We used mainly the RDC randomization, which contains the same total number and type of neurons within the same evaluation area, but randomized gravity centers.

The separate randomization of the diameters (RDD), and of the diameters and the gravity center (RDDC) together, is only used within one cycle of the cluster analytical procedure. We naturally randomized the diameters only in the maximum-minimum range of each population. This was done in order to find out whether the diameters are important components of the cellular arrangement.

$$B_I = d(V_i; V_j) = \sqrt{(X_i - X_j)^2 + (Y_i - Y_j)^2} \quad (1)$$

This general combination provides basic information on the distances between all types of neuron. We therefore included a different tuple in a subprocedure.

The basic distance ($B_I$) can be modified by a distance factor (**f**), and it is possible to change this interactively in the program in order to investigate the pattern formation. The modified distance parameter $L_I$ is calculated with formula (2).

$$L_I = \frac{B_I}{f} \quad (2)$$

We used a planimetric algorithm to estimate the maximum diameter $D_m$. Combined with the second tuple member this gives the sum of the radii of two neurons (3).

$$D_I = \frac{D_{m_i}}{2} + \frac{D_{m_j}}{2} \quad (3)$$

The parameters $L_I$ and $D_I$ were combined in the form of an inequality (4). The inequality can be interpreted as a selection criterium (*C*). *C* becomes true if $D_I$ (3) is equal to or greater than $L_I$ (2). Therefore only those cells of a certain relatively large size and with a relatively small distance were accepted as cluster members.

If the

$$L_I \leqq D_I \quad (4)$$

criterion is fulfilled a tuple is selected.

The variation of **f** defined by the investigator defined for values between 0.6 – 0.8 allows one to determine contact clusters and, for 1.0, to calculate neighbourhood clusters (Schmitt 1991). With these formal tools it is possible to determine different orders of neuron type specific vicinity. Neighbourhood cluster analysis (NCA) is valid with a **f** value of 1.0, whereas contact cluster analysis requires

f = 0.6. This empirical factor determination is based on a visual impression of neuron contact frequencies.

A practical introduction to *point pattern analysis* (PPA) has been given by Diggle (1983). PPA constists of different testing procedures for point or event patterns in bounded or discrete regions. If the points are randomly distributed within a bounded region, this is known as complete spatial randomness (CSR or Poisson process) (Diggle 1983). The second possible point distribution is a cluster or aggregate (cluster process or Matérn cluster process (MCL)). The third possibility is that of regular appearence (hard-core process or Matérn hard-core process (MHC)).

PPA provides methods for analysing these three basic point patterns statistically.

We have used PPA as described by Diggle (1983) with 99 ($p < 0.05$ according to Ambartzumjan et al. (1993, p 320)) simulations for random distributed points (Poisson process) and the calculation of OD. If 1 300 neurons were evaluated in one putamen, the gravity centers of these 1 300 neurons were randomized within each of the 99 simulations, and all distances between the neurons estimated. The result of such a simulation cycle is the empirical distribution function (EDF) (Diggle 1983). The EDF consists of 4 curves (Fig. 1). The thinner curves enclose a random space where the CSR is accepted. The upper is called the upper simulation function (USF), and the lower the lower simulation function (LSF). The middle interrupted line represents the means of all simulations. The observed distances (ODF) are compared with these three CSR characterizing curves. If the ODF lies between the USF and LSF, the CSR hypothesis is accepted (i.e. null hypothesis) (Fig. 1). A significant point aggregation (MCL) is present if the ODF exceeds the USF (Fig. 4). If the ODF lies below the LSF, the arrangement of neurons is regular (MHC) (Stoyan et al. 1987, pp. 146–148)). We used two basic tests from PPA: the H(t) and the G(t) test. The H(t) test checks whether the cell arrangement favours a *general or global* MCL or an MHC. The G(t) test checks in a similiar manner whether the nearest neighbouring cell centers have a certain significant *local* topological distribution.

Testing significance is a very time-consuming randomization process which must be carried out independently for each tuple formation of all putamina with extended typification (n = 14).

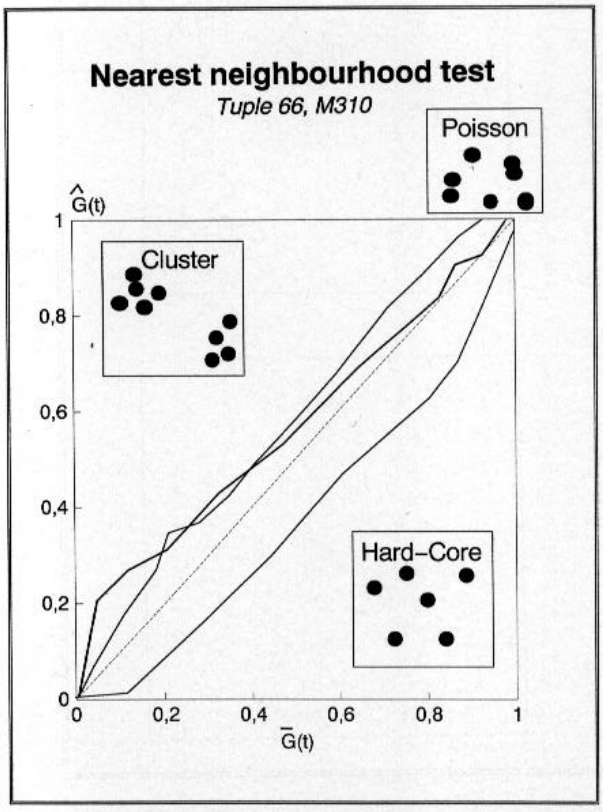


Fig. 1. Graphic representation of a point pattern analysis (PPA) of the neuron type tuple 66 of the human putamen.

## Results

### Visual point field analysis (VPA)

The diagrams in Fig. 2 represent plots of putamina from a 25 (left) and a 100 (right) years-old normal human brain. The plots in Fig. 2a represent a survey on the whole neuron population. In diagram 2b only type 1 neurons have been plotted. The territories of low type 1 neuron frequency are marked in diagram b. In diagram 2c type 6 neurons are shown. Those territories are marked which have a low population of type 1 neurons. The type 6 neurons show a distribution similar to that of the whole field (Fig. 2a). Figure 2d also represents only type 1 neurons, with territories containing a low frequency of type 6 neurons within the type 1 neuron population marked in outline.

Figure 2a appears to confirm the hypothesis of randomly distributed neurons within the striatum put forward by Spiegel (1919); Vogt and Vogt (1920); Foix and Nicolesco (1925); Kemp (1968); Fox et al. (1971); Lu and Brown (1977); Kemp and Powell (1971); Bøttcher (1975) and Tennyson and Marco (1973). If, however, a separating plot of neuron types is drawn, a specific arrangements of the neurons can be recognized.

The VPA's show territories which are nearly free from type 1 neurons, but are covered with neurons of type 6 (Fig. 2b and 2c).

### Nearest neighbourhood analysis (NNA)

Figure 3 shows an NNA diagram of the same two brains as in Fig. 2. Each cell is marked by a point and connected by a line to its nearest neighbour cell.

The NNB chains are a peculiar feature of these connections. They can be simple chains, circular connections and ramifications or combinations of circular ramifications. The shortest chain consists of 2 members (a tuple). We have classified and averaged the nearest cell center distances for all neuron tuple of the brains examined. These data were used to construct the smoothed graphs of a particular neuron tuple. The curves were compared with curves of NNA of pseudorandomized cell gravitation centers (RDC) of equal size (Fig. 4 and 5). A conspicuous difference was found in the type 6 population, which shows an initially steep curve segment and a bimodal distance distribution. These features are not present in the RDC curve of tuple 66.

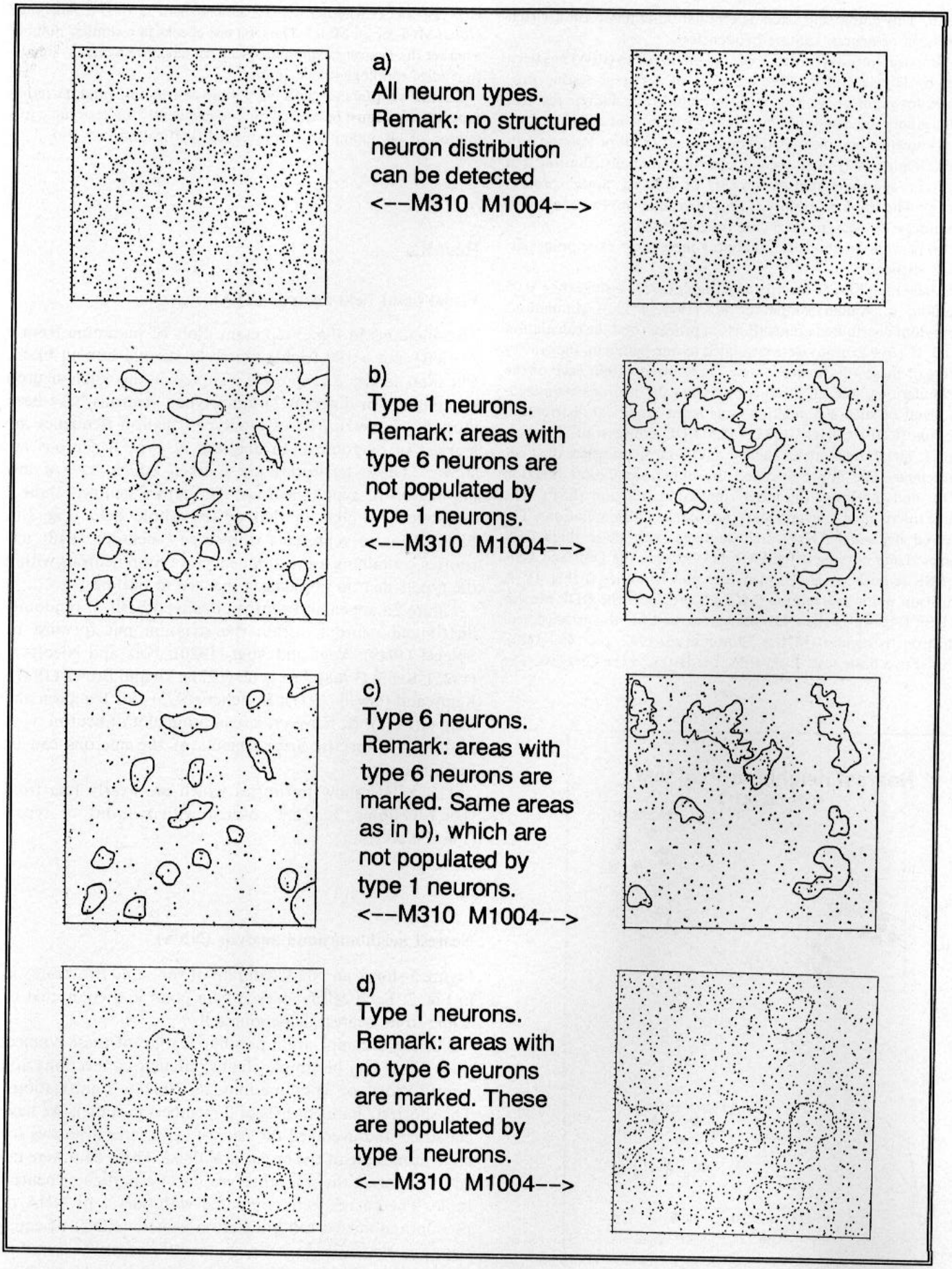


Fig. 2. Graphic representation of a VPA of the human putamen (see text). In order to facilitate comprehension, the scale of the abscissa is 2.5 times that of the ordinate.

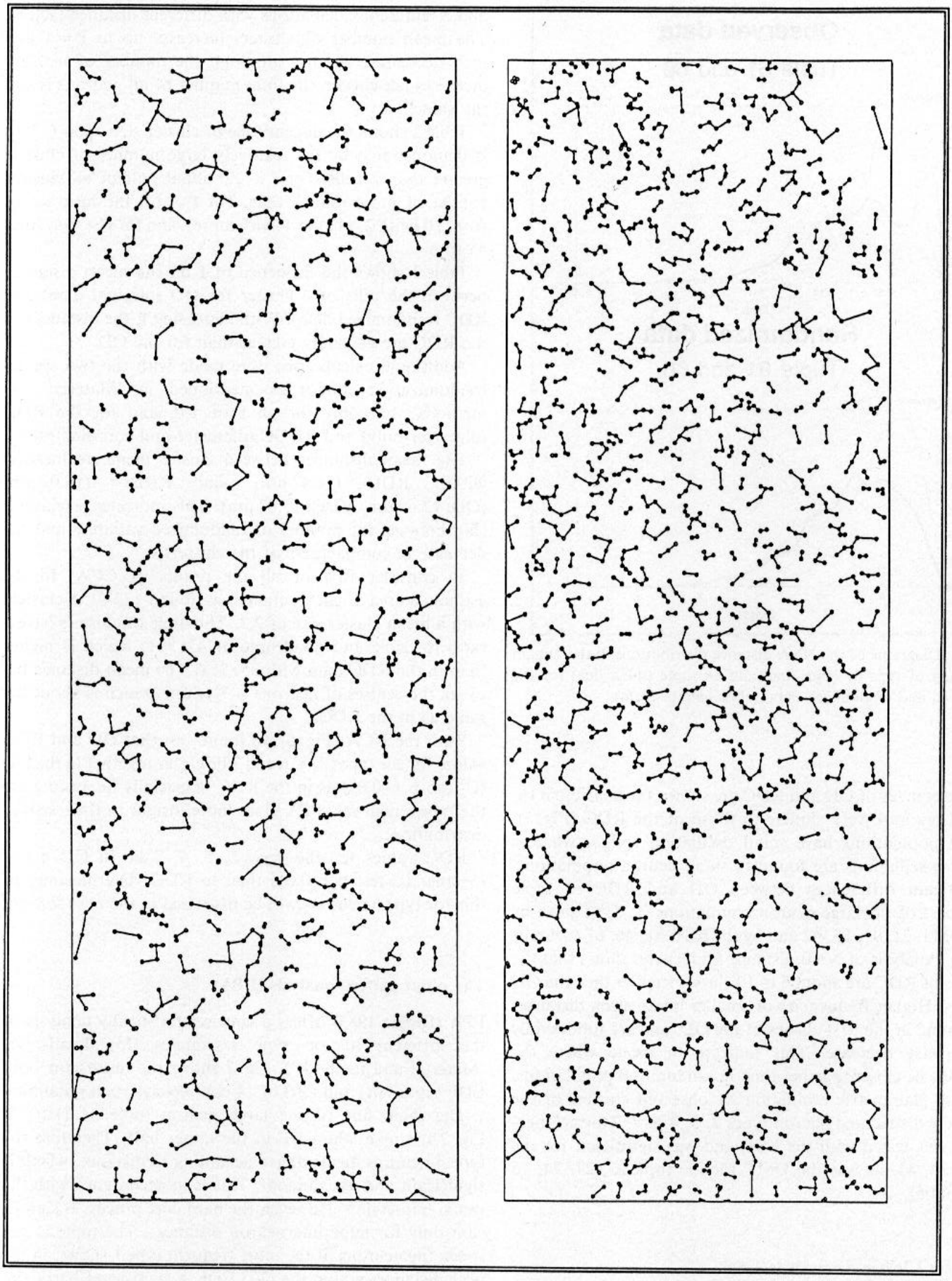

Fig. 3. Graphic representation of an NNA of the human putamen (left: putamen from a 25 year old individual; right: putamen from a 100 year old individual). The abscissa and ordinate are drawn to the same scale.

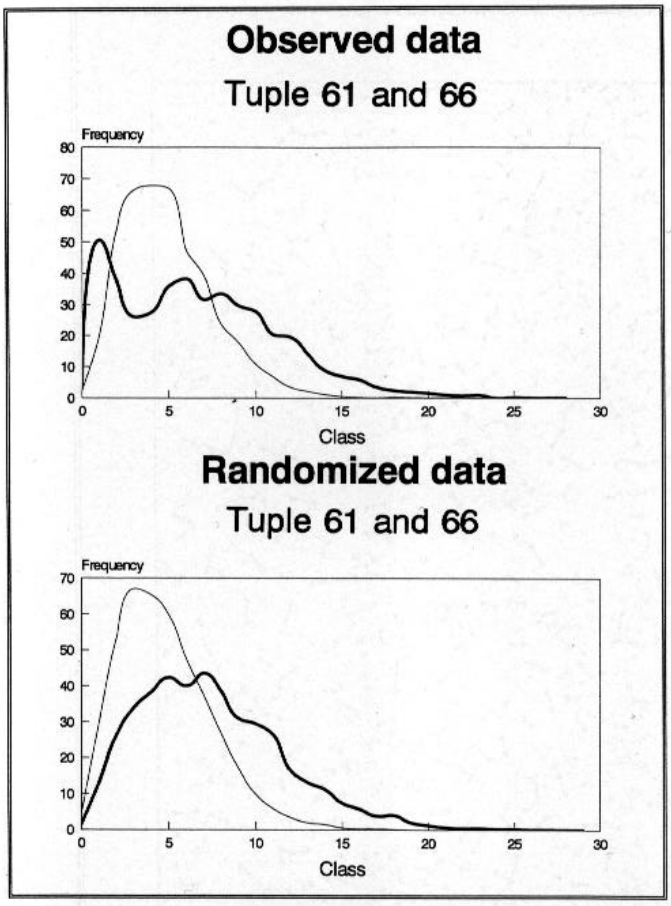


Fig. 4. Diagrams of the NNA distance distributions in the human putamen of type 61 (thin line) and 66 tuple (thick line) for the observed and randomized data. (class length: 5 µm)

The courses of OD and RDC are shown for 6 different tuple. They look very similar to those of the RDC (Fig. 5). Large populations have small oscillation spikes, whereas higher oscillations are found in small neuron populations. Significant differences between OD and RDC of tuple members of the large neuron populations (1, 5, 6) given by the DMT: 21, 41, 55, 62 and by the KST: 41, 46, 61 (Schmitt 1991). Analysis of NNB distance frequencies shows that the curves of RDC are about 5 to 10 classes smaller then the OD curves. Higher frequencies of smaller interneuron distances are found in the first classes of the OD, and are followed by a stepwise decrease. This indicates a tissue where the neurons lie closer together than in randomized populations. During planimetric evaluation we observed clusters of the sparsely distributed neuron types 2, 3, 4 or 7. This arrangement was tested with the KST, and was significant for the tuple 32, 43, as was the DMT for the tuple 23, 27, 74, 75 ($p < 0.05$).

### Contact Cluster Analysis (CCA)

NNA cannot take into account the direct geometrical relation and contact between neurons. We therefore used cluster analysis (CA) with a distance factor **f**. Tables 1, 2 and 3 represent calculations with different distance factors. The mean number of clusters increases up to $\mathbf{f} = 1$ and then decreases, because although the number of neurons increases per cluster, the total number of all neurons is still the same.

Table 2 shows the dependence of cluster size upon **f**. This is demonstrated by the relatively large number of clusters greater than 2 cells. For $\mathbf{f} = 2.0$ about half of all clusters consist of more than 2 cells. For $\mathbf{f} = 1.0$ the ratio varies from 10 (with 2 cells) to 4 (with more), and for $\mathbf{f} = 0.6$, from 45 to 6.

Table 3 shows the influence of **f** on the mean distances between the cells of a cluster for OD (original data) and RDC (randomized data). With increasing **f**, the distances of the RDC are generally greater than for the OD.

Additional calculations were made with the two special randomization modes as mentioned in 'Material and methods', but only for an **f** of 1.0, and for the RDD (diameter only) and RDDC (diameter and coordinates).

The mean distances between cluster members increase within RDD (14.47 µm) and RDDC (16.02 µm) (OD: 12.69 µm, RDC: 13.07 µm). This indicates a relationship between the number of randomized variables and the decrease in compactness of the clusters.

To consider first of all the results of CCA: In the estimated area of each putamen we found 122 CCA-clusters with a mean cluster size of 2.2. The tuple of clusters have a ratio to triple and quadruple of 45:5:1, which is higher than in the RDC data with 35:5:1. The mean distance between the centres of neurons is 7.44 µm, which is about the same as in the RDC.

With the NCA (Fig. 6) we found out that OD and RDC values for the types 2, 5, 6 and 7 lie closer together in the OD (U-test: $p < 0.01$) as in the RDC. Especially interesting are the type 6 neurons. PPA gives more insight in their spatial distribution.

RDC values for the types 2, 5, 6, 7 lie in OD closer together (U-test $p < 0.01$) than in RDC. The meaning of this for type 6 neurons will be discussed in the next section.

### The point pattern analysis (PPA)

PPA (Diggle 1983) offers a concise statistically analysis of the different neuron type assemblies (for details see 'Material and methods'). Fig. 7 shows the results for both EDF types H(t) and G(t) of 14 completely typed putamina.

The thick line of the large neuron tuple 44 (H(t) in Fig. 7a) crosses the LDF in the upper half. Therefore the type 4 neurons are arranged according to distance, which is significant and not random. This is in accordance with the visual impression. However, the hard core process is significant only for large interneuron distances. The tuple 11 between the neurons of the most frequent type 1 shows, in the near distances within the G(t) EDF, a significant hard-core process. This means that the distances from cells of this type to other cells of the same type is greater than that predicted by CSR.

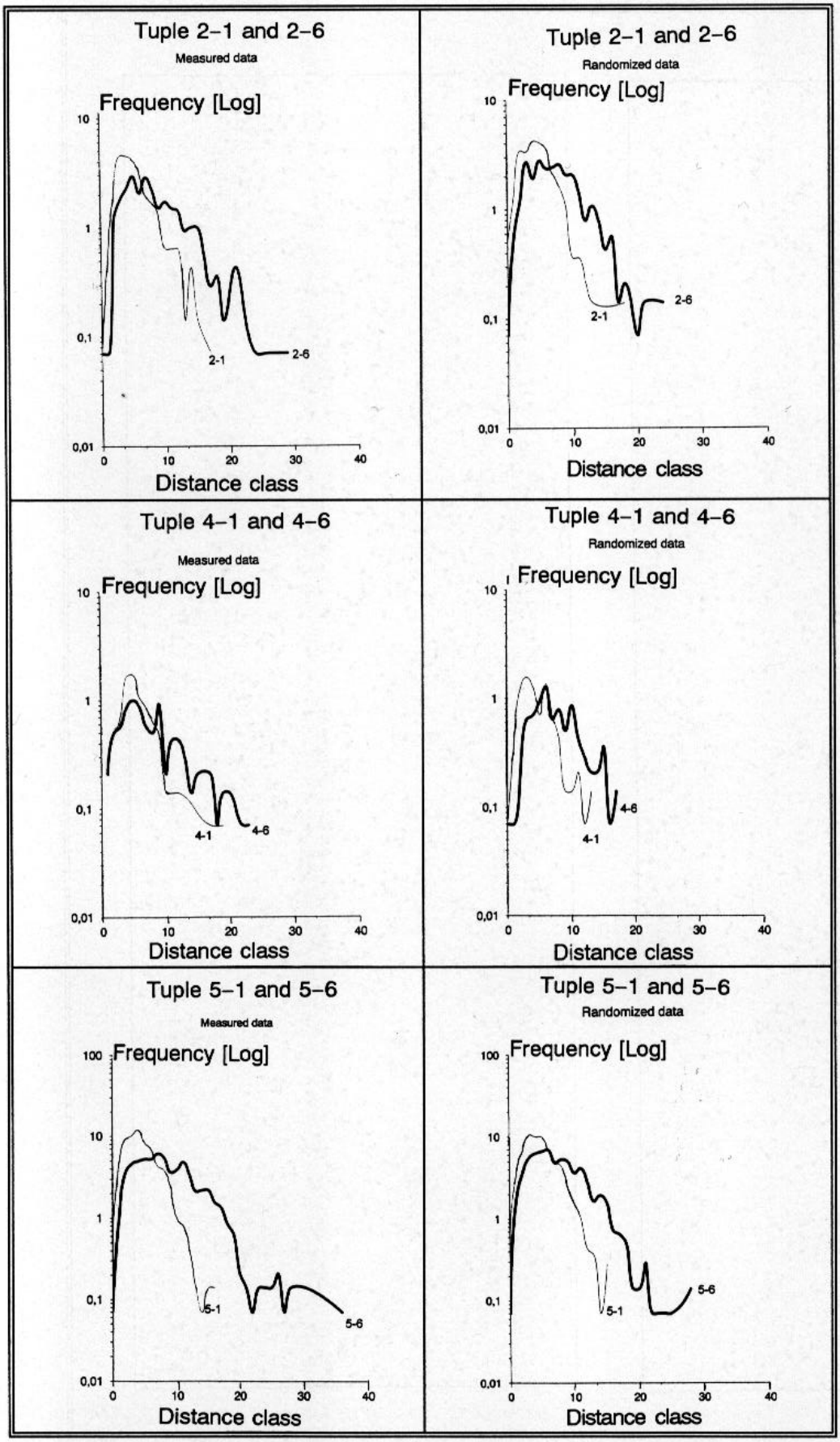


Fig. 5. Diagrams of the NNA distance distributions in the human putamen. (class length: 5 μm)

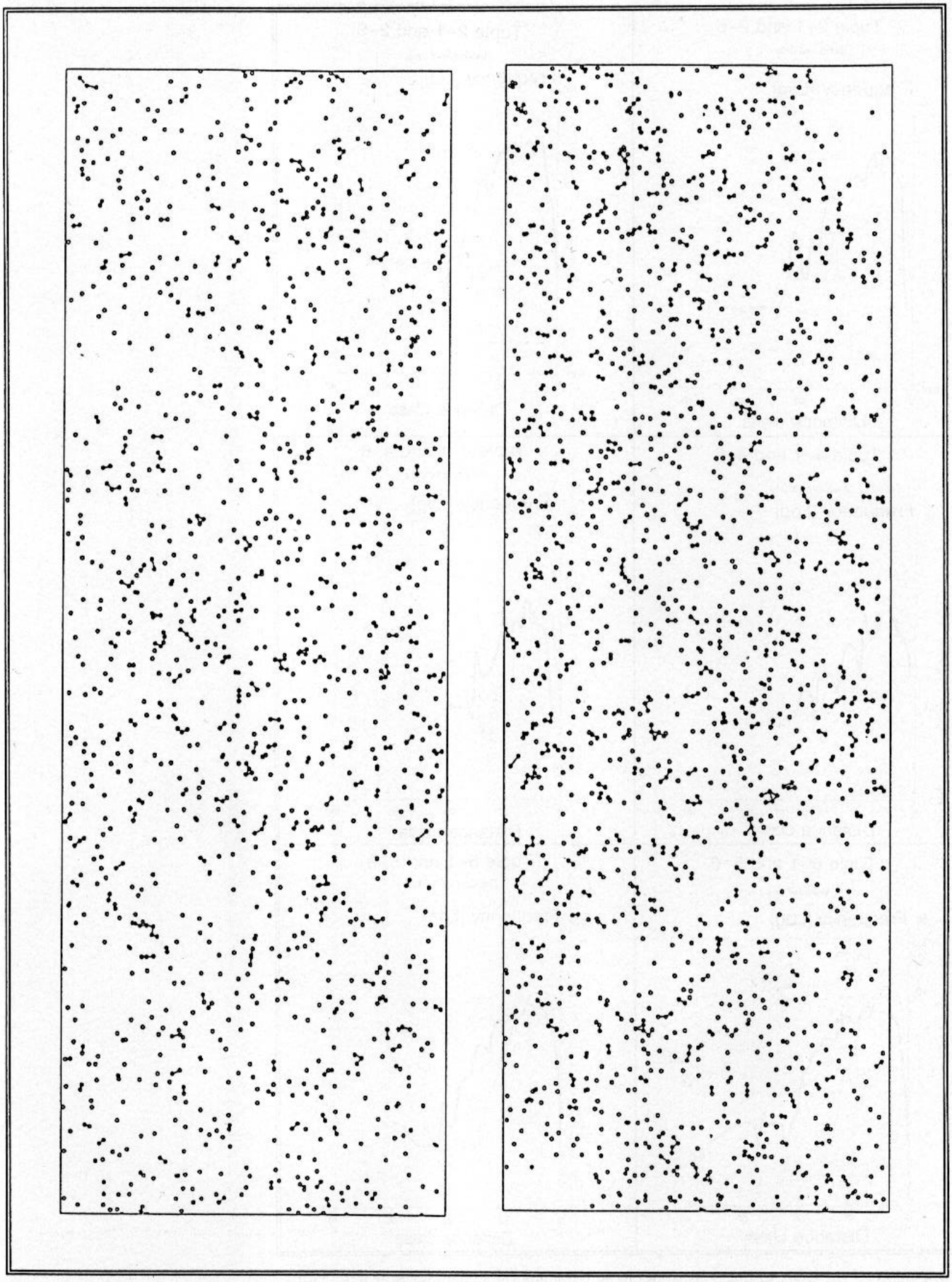

Fig. 6. Graphic representation of an NCA of the human putamen (left: putamen from a 25 year old individual; right: putamen from a 100 year old individual).

Table 1. Result of the cluster analytical method with different values of **f**. The mean number of cluster elements is for **f** = 2.0 higher than the neuron number, because one neuron can be connected to serveral others.

| f | mean number of clusters | mean number of cluster elements | mean cluster size | mean frequency of cluster elements to all neurons |
|---|---|---|---|---|
| 2.0 | 246.0 | 2826.4 | 6.7 | 241.0 |
| 1.0 | 291.2 | 891.4 | 2.5 | 56.0 |
| 0.8 | 216.3 | 524.4 | 2.4 | 33.4 |
| 0.6 | 121.9 | 263.4 | 2.2 | 17.9 |

Table 2. Dependence of ratios of mean normalized cluster size frequencies upon variations in **f**.

| f | modus | cluster size ratios 2 | 3 | 4 |
|---|---|---|---|---|
| 2.0 | OD | 3 | 2 | 1 |
| | RDC | 3 | 1 | 1 |
| 1.0 | OD | 10 | 3 | 1 |
| | RDC | 9 | 3 | 1 |
| 0.8 | OD | 21 | 4 | 1 |
| | RDC | 12 | 3 | 1 |
| 0.6 | OD | 45 | 5 | 1 |
| | RDC | 35 | 5 | 1 |

Table 3. Summary of the main results of the clusteranalysis with different values of **f** and different randomization modes (mean values). **D** is the Euclidean distance in µm. **C** is the mean diameter of connected neurons and **C/t** is the quotient of C and section thickness.

| f | OD D | C | C/t | RDC D | C | C/t |
|---|---|---|---|---|---|---|
| 0.6 | 7.44 | 16.77 | 0.92 | 7.53 | 17.76 | 0.97 |
| 0.8 | 10.04 | 17.06 | 0.94 | 12.36 | 19.80 | 1.08 |
| 1.0 | 12.69 | 17.20 | 0.94 | 13.07 | 17.60 | 0.95 |
| 2.0 | 25.57 | 17.09 | 0.94 | 40.66 | 17.17 | 0.94 |
| | RDD | | | RDDC | | |
| 1.0 | 14.47 | 19.53 | 1.07 | 16.02 | 19.62 | 1.07 |

The type 6 neurons in Fig. 7c show quite different behavior, because their ODF lies significantly above the statistical border. This means that type 6 neurons are associated with small intercellular distances. We have seen in the CCA analysis another expression of the same fact, also in accordance with the visual impression. The PPA is therefore able to discriminate statistically between different distribution functions.

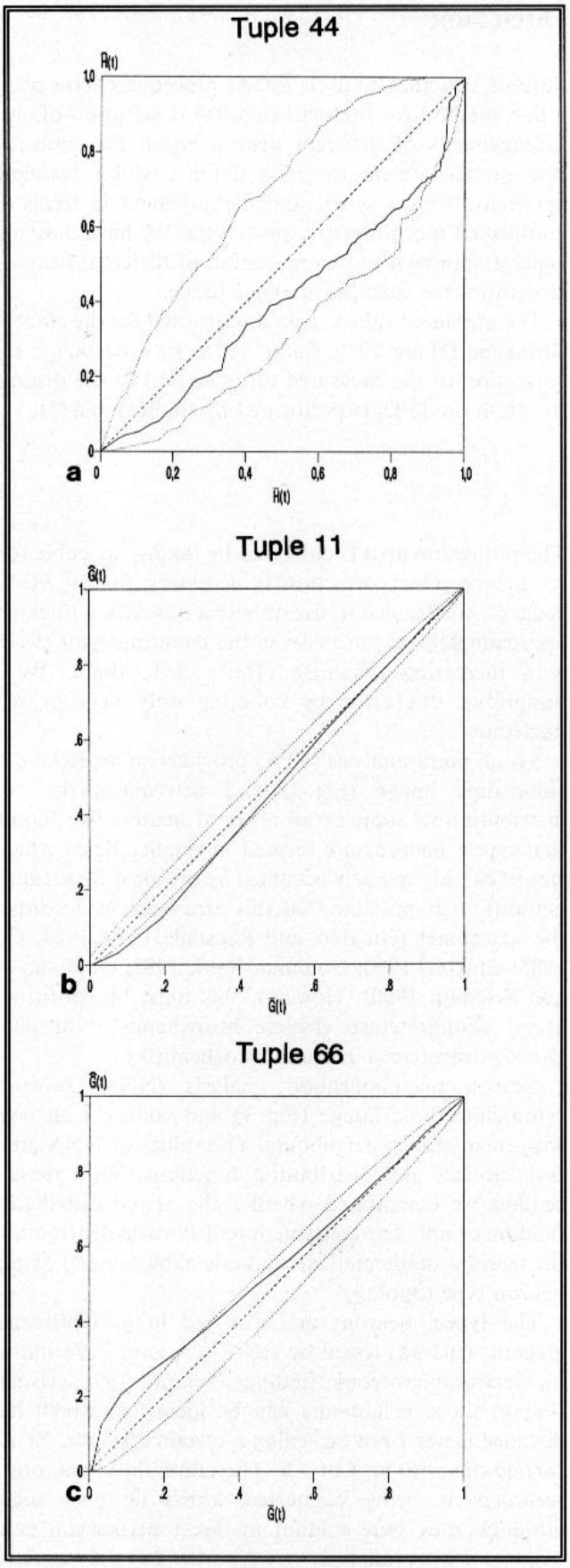


Fig. 7. Point pattern analysis diagrams of the human putamen. Every process has been tested in each of 99 simulations ($p < 0.05$). The sample size is 14.
a: general H(t) test. b, c: local G(t) test. For more details see text.

## Discussion

Various structure analysis (SCA) procedures have provided a new method for the mathematical description of specific arrangements of different neuron types. Prerequisites for this method are the use of a staining which distinguishes between different types, and measurement in terms of an established morphometric procedure. We have developed a general approach to the evaluation of different histological structures; for example, nervous tissue.

The measured values must be corrected for the embedding shrinkage (Haug 1979; Sass 1982a, b). The factor $R_T$ for correction of the measured distance ($D_I$) to the distance in the fresh tissue $D_i$ is performed by the formula (5).

$$\overline{D}_I = \frac{D_i}{\sqrt[3]{R_T}} \qquad (5)$$

The projection area is corrected by taking the cubic root of its square. This correction is necessary for all SCA-procedures. We decided to use only sections with a thickness of approximately 20 µm because the counting error decreases with increasing thickness (Treff 1963, 1967). We have minimized this error by counting only neurons with a nucleolus.

Visual point analysis (VPA) provides an artificial cytoarchitectonic image (Fig. 2) and determines the correct distribution of some or all types of neuron. We found out that type 6 neurons are located in smaller fields which are free of or only sparsely occupied by the most frequent type 1 neurons. It is possible that this arrangement accords with the striosomes (Graybiel and Ragsdale 1978, 1983; Gerfen 1985; Graybiel 1990; Goldman-Rakic 1982; Goldman-Rakic and Selemon 1990). However, this must be confirmed by acetyl cholinesterase enzyme histochemistry or choline-O-acetyltransferase immunohistochemistry.

Nearest neighbourhood analysis (NNA) provides a cytoarchitectonic image (Fig. 3) and connects all neurons with their nearest neighbours. The values of NNA are used for statistics and distribution functions. With these procedures we determined whether the actual distribution is random or not. The construction of Poisson distributions by the relevant mathematical methods allows one to assess the neuron type topology.

The type 6 neurons are arranged in a significant aggregate. This was tested by NNA, CA, and PPA and based on electronmicroscopic findings (Schmitt 1991). Using CA (Fig. 6) those neighbours can be identified which have a distance factor **f** not exceeding a certain distance. NCA was carried out with an **f** of 1.0. Therefore, those neurons were regarded as being connected which lie near together, although they were seldom in direct perikaryon contact. Contact cluster analysis (CCA) with **f** = 0.6 restricts the distance to a value in which the contact of cell body with cell body is probable. For the type 6 neurons, CCA reveals a number of contacts. One problem is that the neurons can be situated near the upper or lower border of the histological section. Without direct contact, their gravity points might lie within an **f** of 0.6. In our experience these cases are rare. Table 3 shows that the relevant mean diameters lie within the section thickness.

For obtaining more information about type relations, the mathematical terminus tuple proved to be useful. A tuple consists of two neurons and is named after the number of each type. A tuple with equal numbers consits of neurons of the same type.

Point pattern analysis (PPA) is, even for a fast PC, a time-consuming method, since it is based on estimations of all distances between the neurons. With the PPA methods one obtains information if the relevant neurons are concentrated in clusters, regularly (Matérn hard-core process) or randomly distributed (Poisson process). The type 4 neurons have a tendency to lie in regular formation at large intercellular distances. This can be seen more clearly within the population of type 1 neurons, which however involves only the smaller distances. On the other hand, the type 6 neurons have a tendency to lie in clusters close together.

The special arrangements of type 6 and type 1 neurons make it possible to survey the SCA-procedures which were used. With NNA, CCA and PPA, they reveal a special feature, which is the aggregation of smaller clusters, with perikaryon to perikaryon contact (type 6 neurons) or 'keeping their distance' (type 1 neurons).

The influence of certain border sizes on SCA results will be examined in the near future. We also hope to develop SCA methods and speed up computation time (Preparata and Shamos 1985; Moret and Shapiro 1991; Chen et al. 1992; Saxl 1993) in 3 dimensions, in order to get more insight into structural relationships of the neuronal cytoarchitecture.

## References


Ambartzumjan RV, Mecke J, Stoyan D (1993) Geometrische Wahrscheinlichkeiten und Stochastische Geometrie. Akademie Verlag, Berlin

Benes FM, Matthysse SW, Davidson J, Bird ED (1987) The spatial distribution of neurons and glia in human cortex based on the Poisson distribution. Ann Quant Cytol Histol 9: 531–534

Böker F (1987) Über statistische Methoden bei Punktprozessen. Verlag Otto Schwartz & Co., Göttingen

Bøttcher J (1975) Morphology of the basal ganglia in Parkinson disease. Acta Neurol Scand Suppl 52: 7–87

Braendgaard H, Gundersen HJG (1987) The impact of recent stereologic advances on quantitative studies of the nervous system. J Neurosci Meth 18: 39–78

Chen YA, Lin YL, Chang LW (1992) A systolic algorithm for the k-nearest neighbors problem. IEEE Trans Comp 41: 103–108

Davis JC, McCullagh MJ (1975) Display and analysis of spatial data. John Wiley & Sons, London

Diggle PJ (1983) Statistical analysis of spatial point patterns. Academic Press, London

Eggers R (1984) Präparative Einflüsse auf das Schrumpfungsverhalten und das mikroskopische Bild von Gehirngewebe. Verh Anat Ges 78 (Anat Anz Suppl 156): 529–531

Foix C, Nicolesco J (1925) Les noyaux gris centraux et la région mésencéphalo-sous-optique. Paris, pp. 296–298

Fox CA, Andrade AN, Hillman DE, Schwyn RC (1971) The spiny neurons in the primate striatum: a Golgi and electron microscopic study. J Hirnforsch 13: 341–201

Getis A, Boots B (1978) Models of spatial processes. Cambridge University Press, London

Gerfen CR (1985) The neostriatal mosaic. I. Compartmental organization of projections from the striatum to the substantia nigra in the rat. J Comp Neurol 236: 454–476

Goldman-Rakic PS (1982) Cytoarchitectonic heterogeneity of the primate neostriatum: Subdivision into island and matrix cellular compartments. J Comp Neurol 205: 398–413

Goldman-Rakic PS, Selemon LD (1990) New frontiers in basal ganglia research. TINS 13: 241–244

Graybiel AM, Ragsdale CW (1978) Histochemically distinct compartments in the striatum of human monkey and cat demonstrated by acetylcholinesterase staining. Proc Natl Acad Sci USA 75: 5723–5726

Graybiel AM, Ragsdale CW (1983) Biochemical anatomy of the striatum. In: Emson PC (ed) Chemical neuroanatomy. Raven Press, New York, pp 427–504

Graybiel AM (1990) Neurotransmitters and neuromodulators in the basal ganglia. TINS 13: 244–254

Harding EF, Kendall DG (1974) Stochastic geometry. John Wiley & Sons, London

Haug H (1979) The evaluation of cell-densities and of nerve-cell-size distribution by stereological procedures in a layered tissue (cortex cerebri). Microsc Acta 82: 147–161

Karr AF (1991) Point processes and their statistical inference. Marcel Dekker, New York

Kemp JM (1968) An electron microscopic study of the termination of afferent fibres in the caudate nucleus. Brain Res 11: 464–467

Kemp JM, Powell TPS (1971) The structure of the caudate nucleus of cat: light and electron microscopy. Philos Trans R Soc Lond Biol 262: 383–401

König D, Schmidt V (1992) Zufällige Punktprozesse. Teubner, Stuttgart

Lu EJ, Brown WJ (1977) The developing caudate nucleus in the euthyroid and hypothyroid rat. J Comp Neurol 171: 261–284

Mariani AP, Kolb H, Nelson R (1984) Dopamine-containing amacrine cells of rhesus monkey retina parallel rods in spatial distribution. Brain Res 322: 1–7

Matérn B (1960) Spatial variation. Meddelanden från Statens Skogsforskningsinstitut 49: 1–44

Mecke J, Schneider RG, Stoyan D, Weil WRR (1990) Stochastische Geometrie. Birkhäuser, Basel

Moret BME, Shapiro HD (1991) Algorithms from P to NP. Volume I. The Benjamin/Cummings Publishing Company, Redwood City, pp 444–451

Preparata FP, Shamos MI (1985) Computational geometry. An introduction. Springer, New York, pp 195–204

Ranke TP, Ranke I, Schwandtke A, Rother P (1989) Quantitative Analyse von Chondrocytenverteilungsmustern im hyalinen Knorpelgewebe – Vergleich verschiedener Modelle. Gegenbaurs Morphol Jahrb 135: 125–131

Rogers A (1974) Statistical analysis of spatial dispersion. Pion Limited, London

Rother P, Stoyan D, Ranke TP, Ranke I, Kreutz W (1987) Quantitative Analyse des Chondrocytenverteilungsmusters im transitorischen hyalinen Knorpel der embryonalen Anlage von Sternum und Patella. Z mikrosk anat Forsch 101: 69–78

Saß NL (1982a) Altersabhängige Veränderungen im Gyrus rectus des Menschen nach dem 35. Lebensjahr. Medical dissertation, Medical University of Lübeck

Saß NL (1982b) The age-dependent variation of the embedding shrinkage of neurohistological sections. Mikroskopie 39: 278–281

Saxl I (1993) Contact distances and random free paths. J Microsc 170: 53–64

Schmitt O (1991) Die Cytoarchitektonik des menschlichen Putamen. Eine qualitative und quantitative Typisierung der Neuronen, ihre Altersveränderungen sowie Analyse zweidimensionaler Verteilungen. Medical dissertation, Medical University of Lübeck.

Schmitt O, Eggers R, Haug H (1995) Quantitative investigations into the histostructural nature of the human putamen. I Staining, cell classification and morphometry, Ann Anat, in press

Spiegel E (1919) Die Kerne im Vorderhirn der Säuger. Arb neurol Inst Wien Uni 22: 418–497

Stoyan D, Kendall WS, Mecke J (1987) Stochastic geometry and its applications. John Wiley & Sons, Chichester

Stoyan D (1993) Stochastik für Ingenieure und Naturwissenschaftler: Eine Einführung in die Wahrscheinlichkeitstheorie und mathematische Statistik. Akademie Verlag, Berlin

Tautu P (1984) Stochastic spatial processes in biology: a concise historical survey. In: A Dold, B Eckmann (eds) Lecture notes in mathematics, Stochastic spatial processes, Mathematical theories and biological applications proceedings, Heidelberg 1984. Springer, Berlin, p 1212

Tennyson VM, Marco LA (1973) Intrinsic connections of caudate neurons. II. Fluorescence and electron microscopy following chronic isolation. Brain Res 53: 307–317

Treff W (1963) Einfluß der Schnittdicke auf die meßbaren Größen bei Nervenzellen. First International Congress for Stereology, Vienna, April 18–20, 18/1–18/12

Treff W (1967): Zur Methodik der Zellzählung an subcortikalen Strukturen des menschlichen Gehirns. In: Weibel ER, Elias H (eds) Quantitative Methoden in der Morphologie. Springer Heidelberg, pp 79–86

Upton G, Fingleton B (1985) Spatial data analysis by example. Point pattern and quantitative data, Vol. 1. John Wiley & Sons, Chippenham

Vogt C, Vogt O (1920) Zur Lehre der Erkrankungen des striären Systems. J Psychol Neurol 25: 651–655

Accepted January 12, 1995